

## Exponential improvement of the sign problem via contour deformations in the 2+1D XY model at non-zero density

---

Matteo Giordano,<sup>a</sup> Kornél Kapás,<sup>a</sup> Sándor Katz,<sup>a,b</sup> Attila Pásztor<sup>a</sup> and Zoltán Tulipánt<sup>a,\*</sup>

<sup>a</sup>*Eötvös Loránd University, Institute for Theoretical Physics, Pázmány Péter sétány 1/A, H-1117, Budapest, Hungary*

<sup>b</sup>*MTA-ELTE Theoretical Physics Research Group, Pázmány Péter sétány 1/A, H-1117 Budapest, Hungary*

E-mail: [tulipantz@staff.elte.hu](mailto:tulipantz@staff.elte.hu)

We studied the 2+1 dimensional XY model at nonzero chemical potential on deformed integration manifolds with the aim of alleviating its sign problem. We investigated several proposals for the deformations and managed to considerably improve on the severity of the sign problem with respect to standard reweighting approaches. In this talk I present numerical evidence that a significant reduction of the sign problem can be achieved which is exponential in both the squared chemical potential and the spatial volume. Furthermore, I discuss a new approach to the optimization procedure, based on reweighting, that sensibly reduces its computational cost.

*The 39th International Symposium on Lattice Field Theory,  
8th-13th August, 2022,  
Rheinische Friedrich-Wilhelms-Universität Bonn, Bonn, Germany*

---

\*Speaker

## 1. Introduction

Introducing a non-zero chemical potential in a euclidean quantum field theory the path integral weights become complex and therefore cannot be interpreted as Boltzmann weights. In QCD this problem becomes a roadblock for describing neutron stars, supernovae and even heavy ion collisions at low energies with a first-principles approach. In some cases the sign problem can be solved by a reformulation of the theory in different variables, such that in the new variables the weights are manifestly real and positive [1–5]. This has not been achieved in QCD so far.

The existence of this problem does not make simulations completely impossible. They can still be carried out by Monte Carlo methods in the phase-quenched (PQ) theory, with Boltzmann weights proportional to  $|e^{-S}|$ , or the sign-quenched theory, with weights proportional to  $|\text{Re } e^{-S}|$ . After performing such simulations, the expectation value of some operator  $O$  in the original theory can be reconstructed via reweighting

$$\langle O \rangle = \frac{\langle O e^{i\theta} \rangle_{PQ}}{\langle e^{i\theta} \rangle_{PQ}} = \frac{\left\langle O \frac{\cos \theta}{|\cos \theta|} \right\rangle_{SQ}}{\left\langle \frac{\cos \theta}{|\cos \theta|} \right\rangle_{SQ}}, \quad (1)$$

where  $\theta$  is the phase of the complex path integral weight, i.e.,  $e^{-S} = |e^{-S}| e^{i\theta}$ . However, large fluctuations in the phase factor lead to large cancellations. We refer to this as a sign problem and quantify its severity with the average phase factor  $\langle e^{i\theta} \rangle$  or the average sign of the real part of the phase factor  $\langle \text{sgn}(\cos \theta) \rangle$ . As long as these quantities are under numerical control one can reconstruct expectation values in the desired theory reliably. Reweighting from phase- and sign-quenched theories is starting to become feasible in QCD [6–9], although the range of applicability is severely constrained by the sign problem, which requires an exponential increase of the statistics both as a function of the volume and of the chemical potential.

In most cases of interest, the path integral weights are holomorphic functions of the fields, thus any integration manifold that is in the same homology class as the undeformed manifold leads to the same partition function [10]. However, the integrands of the phase- and sign-quenched partition functions are not holomorphic. Therefore, it could be possible to ameliorate the sign problem by deforming the integration contours.

We used contour deformations in the 2 + 1D XY model to reduce the severity of the sign problem. Our choice of the model was mainly motivated by the fact that it shares some technical features with QCD, so that we may obtain insight in how to proceed with more complicated theories.

## 2. Contour deformations for the 2 + 1D XY model

The action of the 2 + 1D XY model at non-zero chemical potential [11–13] is given by

$$S = -\beta \sum_x \sum_{n=0}^2 \cos(\varphi_x - \varphi_{x+\hat{n}} + i\mu\delta_{n0}), \quad (2)$$

where the sum goes over all lattice sites and directions, with 0 identified as the temporal direction. Periodic boundary condition is imposed in every direction. The partition function,

$$Z(\mu) = \int_{-\pi}^{\pi} d\varphi_{000} \cdots \int_{-\pi}^{\pi} d\varphi_{N_0 N_1 N_2} e^{-S} \equiv \int_{\mathcal{M}_0} D\varphi e^{-S}, \quad (3)$$

can be interpreted as a complex contour integral in each field variable with endpoints at  $-\pi$  and  $\pi$ , and thus as an integral over the  $N_0N_1N_2$ -dimensional manifold  $\mathcal{M}_0 = [-\pi, \pi]^{N_0N_1N_2}$  embedded in  $\mathbb{C}^{N_0N_1N_2}$ . Deformations of the integration manifold leave  $Z(\mu)$  invariant as long as the boundaries remain the same. Denoting the deformed manifold  $\mathcal{M}$  and parametrizing it with real parameters  $t_x$  we have

$$Z(\mu) = \int_{\mathcal{M}} \mathcal{D}\varphi e^{-S} = \int \mathcal{D}t e^{-S_{\text{eff}}}, \quad (4)$$

where the effective action  $S_{\text{eff}} = S - \ln \det J$  is the difference of the action  $S$  and the logarithm of the Jacobian  $\det J$ . Exploiting the reality of the partition function we can write it in a manifestly real form,

$$Z(\mu) = \int \mathcal{D}t \cos S_{\text{eff}}^I e^{-S_{\text{eff}}^R}, \quad (5)$$

where  $S_{\text{eff}}^R$  and  $S_{\text{eff}}^I$  are the real and imaginary parts of the effective action. This enables us to make use of the sign reweighting approach [8, 9, 14, 15] by using the absolute value of the integrand as a weight in importance sampling. The corresponding expectation values will be denoted as  $\langle \dots \rangle_{SQ, \mu}$ . The severity of the sign problem is measured by the average sign,

$$\langle \varepsilon \rangle_{SQ, \mu} \equiv \langle \text{sgn}(\cos S_{\text{eff}}^I) \rangle_{SQ} = \frac{\int \mathcal{D}t \cos S_{\text{eff}}^I e^{-S_{\text{eff}}^R}}{\int \mathcal{D}t |\cos S_{\text{eff}}^I| e^{-S_{\text{eff}}^R}} = \frac{Z}{Z_{SQ}}, \quad (6)$$

which is the ratio of the original and the sign-quenched partition functions. Although the deformation of the integration manifold leaves the numerator unchanged it does alter the denominator, hence it affects the average sign. Our goal is to maximize the average sign using contour deformations. To this end, we introduce various ansätze for the integration manifold and perform gradient ascent with respect to some  $p_i$  coefficients that determine the contours.

We parametrize the integration manifold by the real parts of the field variables on different lattice sites, denoted as  $t_x$ . The imaginary parts of the fields are then expressed as Fourier series in  $t_x$ . As our first attempt, we parametrized each complex  $\varphi_x$  using only the corresponding  $t_x$ , however, the sign problem could not be optimized this way. Using this parametrization the original contour turned out to be a local optimum.

Since the chemical potential affects only the interaction between temporal neighbors directly, it is reasonable to consider including dependence on the nearest temporal neighbor in the parametrization of  $\varphi_x$ . In order to simplify the computation of the Jacobian we used only one neighboring  $t_x$ ,

$$\varphi_x = t_x + i \left\{ A_{0, x_0} + \sum_{k=1}^K \left[ A_{k, x_0} \cos(k(t_x - t_{x+\hat{0}})) + B_{k, x_0} \sin(k(t_x - t_{x+\hat{0}})) \right] \right\}. \quad (7)$$

The Fourier coefficients were allowed to vary with the temporal coordinate  $x_0$  of the field variable, thus allowing the optimization to break temporal translation invariance if needed. We used the choices  $K = 1$  and  $2$  for the truncation of the Fourier series, which we denoted  $(A, B, K = 1)$  and  $(A, B, K = 2)$ , respectively. Performing optimization on a lattice of size  $\Omega \equiv N_0N_1N_2 = 8^3$  for  $\beta = 0.4$  we have found that the sign problem is improved substantially. The initial values of the coefficients were chosen to be zero for the smallest simulated value of  $\mu^2$ , and for each subsequent  $\mu^2$  to be equal to the final values obtained in the previous optimization round.

The coefficients of the constant and sine terms are smaller by two-three orders of magnitude than the coefficients of the cosine terms and they also fluctuate around zero as a function of  $x_0$ , with a standard deviation that is larger than their average. The coefficients of the cosine terms have roughly the same value on every time slice. This remains true at every simulated value of  $\mu^2$ , suggesting there is no gain in allowing for  $x_0$ -dependent Fourier coefficients. Furthermore, carrying out optimization on  $\Omega = 8 \times 4^2$ ,  $8 \times 6^2$  and  $8 \times 10^2$  lattices we have found the same values for the optimal coefficients as the ones obtained on the  $\Omega = 8^3$  lattice.

As a verification we have repeated optimization with the ansatz of Eq. (7) with  $K = 2$ , the coefficients of the constant and sine terms set to zero and  $A_{k,x_0} = A_k$  for all  $x_0$ . This will be denoted as the  $(A_1, A_2)$  optimization and it achieved the same improvement as the previous optimization procedure with optimal coefficients that are in agreement with the ones obtained before.

Including additional neighbors in the parametrization of the field variables the calculation of the Jacobian generally becomes more cumbersome. In order to avoid this additional computational cost we introduced parametrizations with a triangular Jacobian matrix. The first of these ansätze we tested was the one containing nearest spatial neighbors,

$$\varphi_x = t_x + \iota \sum_{k=1}^K \sum_{n=0}^2 \theta_n^{(1)} \left[ \bar{A}_{k,n} \cos(k(t_x - t_{x+\hat{n}})) + \bar{B}_{k,n} \sin(k(t_x - t_{x+\hat{n}})) \right], \quad (8)$$

where

$$\theta_i^{(j)} = \begin{cases} 1 & \text{if } x_i < N_i - j, \\ 0 & \text{otherwise.} \end{cases} \quad (9)$$

This means we constrained the field variables on the slices  $x_i = N_i - 1$  for  $i = 0, 1, 2$  to be independent of the real parts of their neighbors in the  $i$ th direction, thus making the Jacobian matrix triangular at the price of breaking the translational invariance of the parametrization. Except for these points we used the same Fourier coefficients across all lattice sites. This parametrization allows us to assess the consequence of breaking temporal translational invariance and whether the optimal choice of contours is affected by the inclusion of spatial neighbors.

We have also tested the ansatz

$$\varphi_x = t_x + \iota \sum_{k=1}^K \left[ \theta_0^{(1)} a_k \cos(k(t_x - t_{x+\hat{0}})) + \theta_0^{(2)} \cos(k(t_x - t_{x+2\hat{0}})) \right], \quad (10)$$

with two setups: using  $K = 2$  and varying  $a_1$  and  $a_2$  while  $b_k$ s were set to zero, later referred to as  $(a_1, a_2)$  optimization; or using  $K = 1$  and adjusting both  $a_1$  and  $b_1$ , which we refer to as  $(a_1, b_1)$  optimization.

In Fig. 1 we compare optimized results obtained with the parametrizations of Eqs. (8) and (10) with the unoptimized results and with the previously obtained results. Looking at the average sign obtained with Eq. (8) for  $K = 2$  and the  $(a_1, a_2)$  method we can see that the inclusion of spatial neighbors has not led to any significant improvement. In fact, the optimal values of  $\bar{A}_{k,i}$  and  $\bar{B}_{k,i}$  for  $i = 1, 2$  and  $\bar{B}_{k,0}$  are much smaller than those of  $\bar{A}_{k,0}$ , which in turn are in agreement with those obtained for  $A_{k,x_0}$  from the ansatz of Eq. (7). We also see that including the second-order term  $a_2$  for nearest temporal neighbors gives a larger increase for the optimized  $\langle \varepsilon \rangle_{SQ,\mu}$  than including the

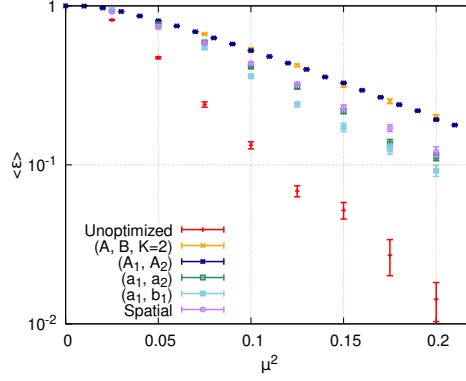


**Figure 1:** Severity of the sign problem on an  $\Omega = 8^3$  lattice with  $\beta = 0.4$ . Unimproved results are shown in red. The optimized results achieved with the parametrizations given in Eq. (7) with  $K = 2$  are shown in orange. The optimization results achieved with Eq. (8) are shown in purple. The result from Eq. (10) with  $a_1$  and  $a_2$  non-zero are shown in green, while with  $a_1$  and  $b_1$  non-zero are shown in light blue. Results with the fully translationally invariant  $(A_1, A_2)$  parametrization are shown in dark blue.

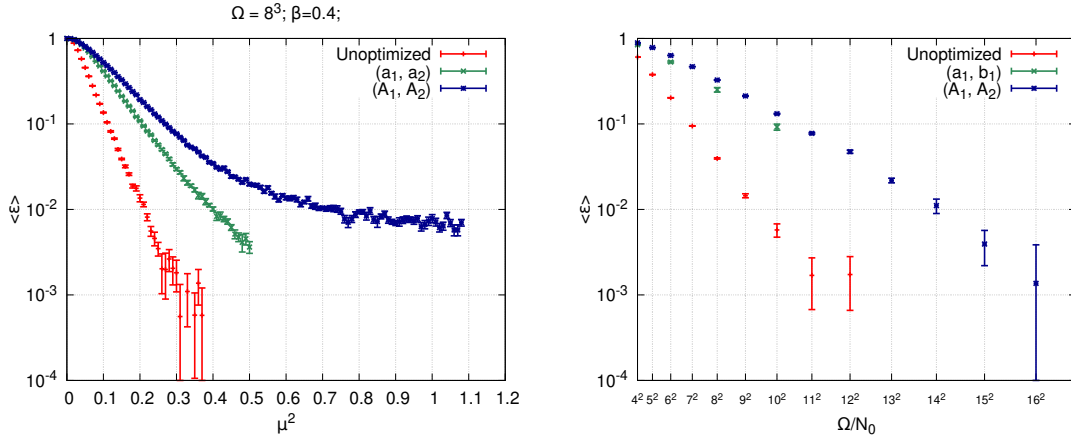


**Figure 2:** Left: Dependence on  $\mu^2$  of the average sign for  $\beta = 0.4$  and  $\Omega = 8^3$  for the unoptimized calculations (red), and the optimized calculations with  $(a_1, a_2)$  (green) and  $(A_1, A_2)$  (blue) parametrizations. Right: Volume dependence of the unoptimized (red),  $(a_1, a_2)$ -optimized (green) and  $(A_1, A_2)$ -optimized (blue) average signs. Results were obtained at  $\beta = 0.4$  and  $\mu^2 = 0.15$  with the temporal size fixed at  $N_0 = 8$ .

first-order term  $b_1$  for next-to-nearest neighbors. Hence it is more important to go to second order in the Fourier series than to include more neighbors in the parametrization.

It is also apparent that the ansätze with a triangular Jacobian matrix lead to a significantly but not overwhelmingly smaller improvement in the average sign compared to the first ansatz of Eq. (7). In the model we used, parametrizations with the triangular Jacobian matrix are not significantly cheaper to simulate than the fully translationally invariant ansatz, so there is no gain in breaking translational invariance due to the sizable difference in the achieved improvement. In other models there might be a less obvious trade-off.

On the left-hand side of Fig. 2 we compare the chemical potential dependence of the average

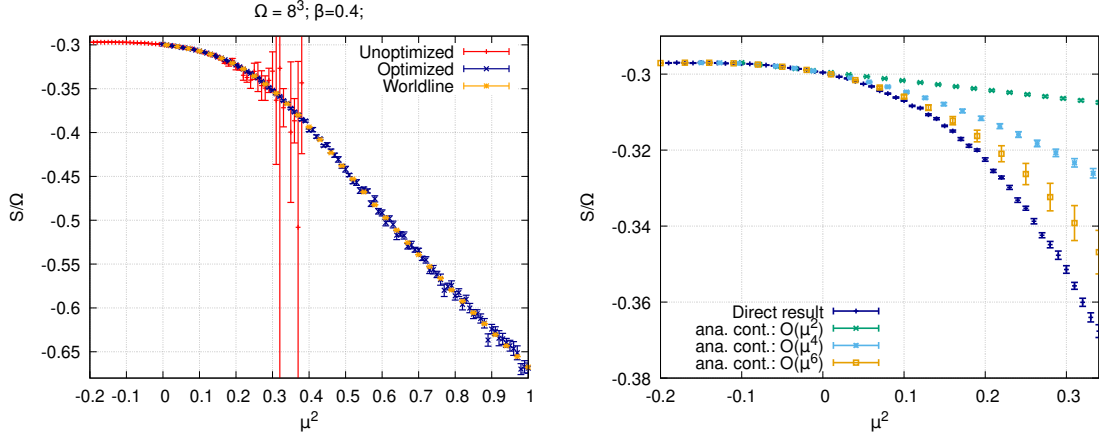


**Figure 3:** Left: Average action density on an  $\Omega = 8^3$  lattice with  $\beta = 0.4$ . The unoptimized results are shown in red, the  $(A_1, A_2)$ -optimized results in blue and the worldline results in orange. Right: Average action density with the  $(A_1, A_2)$ -optimized contours, compared with analytic continuation with polynomial ansätze up to orders  $\mu^2$ ,  $\mu^4$  and  $\mu^6$  for small chemical potentials.

sign with and without optimization for the  $(a_1, A_2)$  and  $(a_1, a_2)$  parametrizations. The ratio of the average sign for the unoptimized case and our best parametrization reaches  $10^2$  at  $\mu^2 = 0.3$  beyond which the unoptimized approach breaks down due to large uncertainties. An exponential fit of the form  $\langle \varepsilon \rangle_{SQ, \mu} \sim e^{-C^{(\mu)} \mu^2}$  in the range  $[0.1, 0.25]$  yields  $C_{\text{unopt}}^{(\mu)} \approx 24$ ,  $C_{(a_1, a_2)}^{(\mu)} \approx 13$  and  $C_{(A_1, A_2)}^{(\mu)} \approx 10$ . The volume dependence of the average sign on the right-hand side of Fig. 2 shows a clear exponential decrease  $\langle \varepsilon \rangle_{SQ, \mu} \sim e^{-C^{(V)} V}$ , with  $C_{\text{unopt}}^{(V)} \approx 0.0073$ ,  $C_{(a_1, a_2)}^{(V)} \approx 0.0032$  and  $C_{(A_1, A_2)}^{(V)} \approx 0.0031$ . The improvement of the sign problem achieved with the best ansatz is exponential in the volume, reducing the volume scaling by 50%.

We have computed the average action density as

$$\frac{\langle S \rangle}{\Omega} = -\beta \frac{\partial}{\partial \beta} \ln Z = \frac{\langle \varepsilon (S^R + S^I \tan S_{\text{eff}}^I) \rangle_{SQ, \mu}}{\Omega \langle \varepsilon \rangle_{SQ, \mu}}, \quad (11)$$

for  $\beta = 0.4$  and  $\Omega = 8^3$ . We present the unoptimized and the  $(A_1, A_2)$  optimized results along with worldline calculations [12] on the left-hand side of Fig. 3. Clearly, reweighting on the optimized manifold outperforms the one done on the unoptimized manifold, allowing us to simulate past the phase transition at  $\mu_c^2 \approx 0.54$  and into the ordered phase while the unoptimized simulation breaks down before reaching  $\mu_c^2$ . On the right-hand side of Fig. 3 we compare the  $(A_1, A_2)$ -optimized reweighting to analytic continuation from  $\mu^2 < 0$  with increasing polynomial order. We observe that the series converges slowly even at small chemical potentials.

### 3. Optimization with reweighting

In order to reduce the cost of the optimization procedure we have introduced a new method based on reweighting. We generate configurations at the start of the optimization and use the same set at every step to compute the gradient of the cost function, reweighting from the original

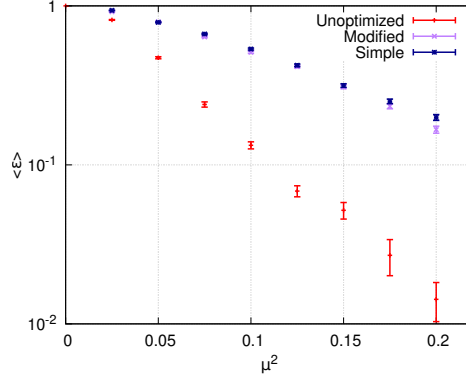


**Figure 4:** Comparison of the average sign achieved with the simple and modified optimization method at  $\beta = 0.4$  and  $\Omega = 8^3$  with the ansatz of Eq. (7).

contour to the updated one. This allows us to save time on the generation of new configurations. Furthermore, computing the gradient of the cost function requires us to evaluate the effective action at every used configuration. Thus, when using a fixed set of sufficiently decorrelated configurations instead of generating a set of similar quality at every step of the procedure also saves time on evaluating the effective action on discarded configurations.

The configurations at the investigated value of  $\mu^2$  are generated using the optimal contour coefficients that were obtained through optimization for the previous value of  $\mu^2$ . When performing the updates at a fixed  $\mu^2$  we reweight from the contour that was used for generating configurations to the one described by the updated values of the contour coefficients. This method can introduce an overlap problem which we need to monitor throughout the entire procedure; should it become too severe we generate a new set of configurations with the current values of the contour coefficients and proceed with the updates. Note that this overlap problem cannot bias the final results, since the original partition function is guaranteed to be the same by the multi-dimensional Cauchy theorem. However, it could lead to a loss in improvement on the sign problem. This is the reason for generating new configurations when the overlap problem in the optimization becomes too severe.

On Fig. 4 we can see that this modified procedure achieved the same improvement as the previously used procedure which required the generation of new configurations at every step. We used the parametrization of Eq. (7). We observed a good agreement between the optimal values of the Fourier coefficients obtained with the two methods. With the new method we had to generate new configurations only twelve times for the eight chemical potentials, which means regeneration took place only four times. Furthermore, the fact that we achieved the same improvement in the sign problem shows that the overlap problem was kept under control well enough to find the optimal contours.

#### 4. Summary

As the severity of the sign problem increases exponentially with both squared chemical potential and volume, improving the performance of reweighting techniques is crucial to gain valuable

information on the phase structure of models with a sign problem. Optimizing the integration manifold of the partition function is a useful tool for achieving a significant improvement. As we have shown on the example of the 2 + 1D XY model, the increase on the average sign with optimization is exponential in both squared chemical potential and volume. This allowed us to simulate even beyond the phase transition and deep into the ordered phase.

We have also introduced a new method based on reweighting which allows us to significantly reduce the computational cost of the optimization procedure. With this method we generate configurations only at the start of the optimization. Then, the same set is used to evaluate the gradient of the cost function at every step. As the contours are updated it is necessary to reweight from the generated distribution to the one corresponding to the updated contours. When the overlap between the two distributions decreases significantly, new configurations must be generated in order to preserve optimizing power. With this method the computation time of the optimization can be greatly reduced without any noticeable loss in the amount of improvement.

## References

- [1] S. Chandrasekharan and U. J. Wiese, *Phys. Rev. Lett.*, vol. 83, pp. 3116–3119, 1999.
- [2] M. G. Alford, S. Chandrasekharan, J. Cox, and U. J. Wiese, *Nucl. Phys. B*, vol. 602, pp. 61–86, 2001.
- [3] M. G. Endres, *Phys. Rev. D*, vol. 75, p. 065012, 2007.
- [4] F. Bruckmann, C. Gattringer, T. Kloiber, and T. Sulejmanpasic, *Phys. Lett. B*, vol. 749, pp. 495–501, 2015. [Erratum: *Phys.Lett.B* 751, 595–595 (2015)].
- [5] C. Gattringer, T. Kloiber, and V. Sazonov, *Nucl. Phys. B*, vol. 897, pp. 732–748, 2015.
- [6] Z. Fodor, S. D. Katz, and C. Schmidt, *JHEP*, vol. 03, p. 121, 2007.
- [7] G. Endrődi, Z. Fodor, S. D. Katz, D. Sexty, K. K. Szabó, and C. Török, *Phys. Rev. D*, vol. 98, no. 7, p. 074508, 2018.
- [8] M. Giordano, K. Kapás, S. D. Katz, D. Nógrádi, and A. Pásztor, *JHEP*, vol. 05, p. 088, 2020.
- [9] S. Borsányi, Z. Fodor, M. Giordano, S. D. Katz, D. Nógrádi, A. Pásztor, and C. H. Wong, arXiv:2108.09213 [hep-lat]
- [10] A. Alexandru, G. Başar, P. F. Bedaque, and N. C. Warrington, arXiv:2007.05436 [hep-lat]
- [11] G. Aarts and F. A. James, *JHEP*, vol. 08, p. 020, 2010.
- [12] D. Banerjee and S. Chandrasekharan, *Phys. Rev. D*, vol. 81, p. 125007, 2010.
- [13] K. Langfeld, *Phys. Rev. D*, vol. 87, no. 11, p. 114504, 2013.
- [14] P. de Forcrand, S. Kim, and T. Takahashi, *Nucl. Phys. B Proc. Suppl.*, vol. 119, pp. 541–543, 2003.
- [15] A. Alexandru, M. Faber, I. Horváth, and K. F. Liu, *Phys. Rev. D*, vol. 72, p. 114513, 2005.